The daughter centriole controls ciliogenesis by regulating Neurl-4 localization at the centrosome

Abdelhalim Loukil, Kati Tormanen, and Christine Sütterlin

Department of Developmental and Cell Biology, University of California, Irvine, Irvine, CA 92697

The two centrioles of the centrosome differ in age and function. Although the mother centriole mediates most centrosome-dependent processes, the role of the daughter remains poorly understood. A recent study has implicated the daughter centriole in centriole amplification in multiciliated cells, but its contribution to primary ciliogenesis is unclear. We found that manipulations that prevent daughter centriole formation or induce its separation from the mother abolish ciliogenesis. This defect was caused by stabilization of the negative ciliogenesis regulator CP110 and was corrected by CP110 depletion. CP110 dysregulation may be caused by effects on Neurl-4, a daughter centriole–associated ubiquitin ligase cofactor, which was required for ciliogenesis. Centrosome-targeted Neurl-4 was sufficient to restore ciliogenesis in cells with manipulated daughter centrioles. Interestingly, early during ciliogenesis, Neurl-4 transiently associated with the mother centriole in a process that required mother–daughter centriole proximity. Our data support a model in which the daughter centriole promotes ciliogenesis through Neurl-4–dependent regulation of CP110 levels at the mother centriole.

Introduction

The centrosome is an asymmetric organelle. In a newly born cell, it is composed of two orthogonally arranged centrioles that are referred to as mother and daughter centrioles. The older mother centriole serves as a platform for the formation of a younger daughter centriole in S phase, leading to an age difference by at least one cell cycle (Conduit et al., 2015). Centrioles are surrounded by pericentriolar material and are connected by cohesion factors, such as LRRC45, Cep68, C-Nap1, and rootletin (Mayor et al., 2000; Bahe et al., 2005; Graser et al., 2007b; He et al., 2013). Centriole age dictates centriole morphology and protein composition, which in turn determines centrosome function and cell organization (Anderson and Stearns, 2009; Sluder and Khodjakov, 2010; Pelletier and Yamashita, 2012).

Most activities of the centrosome are mediated by the mother centriole, which is initially formed as a procentriole, followed by elongation and maturation (Fu et al., 2015). During this maturation process, the older centriole acquires distal and subdistal appendages, which are proteinaceous modifications that are discernible by electron microscopy (Nigg, 2002). Distal appendages are composed of at least five proteins (Cep83, Cep89, Sclt1, FBF1, and Cep164), which are essential for membrane docking during ciliogenesis and the recruitment of the ciliary factor TTBK2 (Graser et al., 2007a; Goetz et al., 2012; Schmidt et al., 2012; Tanos et al., 2013). Subdistal appendages are made up of a different set of proteins that includes ninein, ODF2, and CC2D2A (Delgehyr et al., 2005; Ishikawa et al., 2005; Veleri et al., 2014; Mazo et al., 2016). These proteins control the recruitment of the pericentriolar material as well as the nucleation and anchoring of microtubules. They are also involved in the formation of transition fibers in ciliated cells (Kobayashi and Dynlacht, 2011).

Outside of its role in templating centrosome duplication in S phase (Conduit et al., 2015), only few functions of the daughter centriole have been identified. It lacks obvious appendages, but several proteins appear to be asymmetrically enriched at this younger centriole. These include centrobin, which was found to determine the orientation of the division plate in *Drosophila melanogaster* neuroblasts (Januschke et al., 2013). Neurl-4, another daughter centriole–specific protein, is proposed to prevent the formation of ectopic microtubule organizing centers (Li et al., 2012). The function of additional daughter centriole–enriched proteins, such as PARP-3 and Cep120, are not well understood (Augustin et al., 2003; Mahjoub et al., 2010). Interestingly, the daughter centriole has been implicated in the formation of motile cilia (Al Jord et al., 2014). In multiciliated cells, it is proposed to control ∼90% of the massive centriole amplification that occurs during the differentiation process by promoting the formation of the deuterosome (Al Jord et al., 2014). However, the role of this younger centriole in primary cilia formation has not been tested.

The primary cilium is a prominent hair-like extension of the plasma membrane that is linked to human disease. Present on most differentiated cells, it forms a specialized compartment

Correspondence to Christine Sütterlin: suetterc@uci.edu

Abbreviations used: HFF, human foreskin fibroblast; IF, immunofluorescence; IFT, intraflagellar transport; RPE, retinal pigment epithelial.

The Rockefeller University Press $30.00
J. Cell Biol. Vol. 216 No. 5 1287–1300
https://doi.org/10.1083/jcb.201608119

for signal transduction (Goetz and Anderson, 2010; Hilgendorf et al., 2016). Its membrane, which is continuous with the plasma membrane, has a unique protein composition, being enriched in signaling receptors, such as PTCH, platelet-derived growth factor receptor, and the heterotrimeric transient receptor potential channel (Veland et al., 2009; Goetz and Anderson, 2010; Basten and Giles, 2013). Primary cilia also contain soluble signaling molecules, such as Ca^{2+} and the Gli transcription factors, which are central to the hedgehog pathway (Goetz and Anderson, 2010; Hilgendorf et al., 2016). Defects in cilia formation or dysregulated disassembly of this important signaling "antenna" lead to cell dysfunction and human diseases called ciliopathies. These include rare genetic diseases, such as Bardet–Biedel or Meckel syndrome, as well as common disorders, such as obesity and cancer (Fliegauf et al., 2007; Gerdes et al., 2009).

Ciliogenesis is a multistep process in which the mother centriole plays a fundamental role. Upon cell cycle exit, this older centriole associates with a Golgi-derived ciliary vesicle at its distal end. After fusion of additional vesicles, the mother centriole migrates to the cell surface, where the centriole-associated vesicles fuse with the plasma membrane. The conversion of a docked mother centriole into the basal body and the extension of the ciliary axoneme involves prominent changes in protein composition (Kim and Dynlacht, 2013). For example, components of the intraflagellar transport (IFT) particles, which are necessary for axoneme elongation, are actively recruited to the docked mother centriole (Lechtreck, 2015). In addition, proteins of the transition zone, which describes the region between centriolar appendages and the ciliary axoneme, are brought to the mother centriole (Ishikawa and Marshall, 2011). Furthermore, negative regulators, such as CP110 and its binding partner, Cep97, are removed (Spektor et al., 2007). As CP110 caps the distal ends of centrioles of cycling cells, which prevents untimely cilia formation, its removal from the mother centriole is necessary for basal body formation and axoneme extension (Spektor et al., 2007).

During the cell cycle, CP110 levels are tightly controlled by proteasome-mediated degradation. At least two ubiquitin ligases have been linked to CP110 regulation. The SCF (Skp1–Cul1–F-box) protein ubiquitin ligase and its substrate recognition subunit, the F-box protein cyclin F, are reported to bind CP110 and control its ubiquitylation and degradation (D'Angiolella et al., 2010). The HECT-type E3 ligase HERC2, which is detected at the centrosome, also binds CP110 and was found to control centrosome architecture (Al-Hakim et al., 2012). However, its activity toward CP110 has yet to be demonstrated. The deubiquitinating enzyme USP33 counteracts cyclin F–mediated CP110 degradation and thereby contributes to CP110 regulation (Li et al., 2013). Finally, Neurl-4, which associates with the daughter centriole, is proposed to control CP110 levels to maintain centrosome homeostasis (Li et al., 2012). Although it lacks ubiquitin ligase activity, Neurl-4 overexpression enhances CP110 ubiquitylation (Li et al., 2012). Neurl-4 may function as a substrate recognition factor for HERC2 (Al-Hakim et al., 2012; Martínez-Noël et al., 2012).

In this study, we tested whether the daughter centriole participates in primary cilia formation. Cells in which the younger daughter centriole was either absent or separated from its mother showed stabilized CP110 and ciliogenesis defects that were rescued by CP110 depletion. We also discovered that Neurl-4, a known regulator of CP110, was necessary for ciliogenesis and that its targeting to the centrosome in monocentriolar cells was sufficient to remove CP110 and restore ciliogenesis. Finally, we detected that early during ciliogenesis, Neurl-4 transiently associated with the mother centriole, a process that required mother–daughter centriole proximity and may be necessary for ciliogenesis.

Results

Cells that only contain a mother centriole do not form primary cilia

We examined the spatial relationship between the mother and the daughter centriole in ciliated retinal pigment epithelial 1 (RPE-1) cells. We first serum-starved cells to induce ciliogenesis and then stained them with specific antibodies to the ciliary axoneme (acetylated tubulin), the mother centriole/basal body (Cep164), and the daughter centriole (Neurl-4; Fig. 1 A). The daughter centriole was always adjacent to the basal body, which is derived from the mother centriole. We then compared the distance between the two centrioles in nonciliated and ciliated cells. We detected centrioles with antibodies to glutamylated tubulin, which decorates the centriole wall and thereby avoids issues with centriole orientation (Sonnen et al., 2012). We observed that the distance between the mother and daughter centriole was significantly smaller in quiescent ciliated cells than in cycling nonciliated cells, suggesting a possible link between ciliogenesis and the proximity between the two centrioles (Figs. 1 B and S1 A).

To test this hypothesis, we examined ciliogenesis in monocentriolar cells, which were generated by depleting RPE-1 cells of the centrosome duplication factor HsSAS-6. After progression through mitosis, 37% of HsSAS-6–depleted cells were monocentriolar (Fig. S1 B). We then incubated these cells for 30 h in the absence of serum to induce ciliogenesis (Fig. 1 C), which increased the percentage of monocentriolar, HsSAS-6–depleted cells to 46% compared with 4% of control cells (Fig. S1 B). The single remaining centriole was a mother centriole, because it contained the mother centriole–specific marker Par6G (Dormoy et al., 2013; Fig. S1 C). 61% of control siRNA-transfected cells had two centrioles and formed a primary cilium. In contrast, this cell surface protrusion was only present on 9% of HsSAS-6–depleted cells with a single centriole (Fig. 1 D). This ciliogenesis defect was not caused by a lower confluency of HsSAS-6–depleted cells, which displayed a growth rate similar to control cells (Fig. S1, D and E). It was also not caused by the specific absence of HsSAS-6, because ciliation defects were also observed in monocentriolar cells generated through the depletion of the centriole duplication factor Cep152 (Fig. 1 E). The finding that monocentriolar cells with only a mother centriole were unable to form primary cilia suggests a possible role of the daughter centriole in cilia formation. These results are consistent with the reported absence of primary cilia from cells depleted of STIL or CPAP, two other regulators of centrosome duplication (Wu and Tang, 2012; David et al., 2014).

We next tested if the absence of cilia from monocentriolar cells was caused by an arrest in the G1 phase of the cell cycle. Loss of centrosome integrity is reported to produce an irreversible p53- and p38-dependent cell cycle arrest in G1 (Mikule et al., 2007; Wong et al., 2015). Our experimental conditions did not appear to activate this centrosome integrity checkpoint. In the time frame of our experiment, HsSAS-6–depleted cells

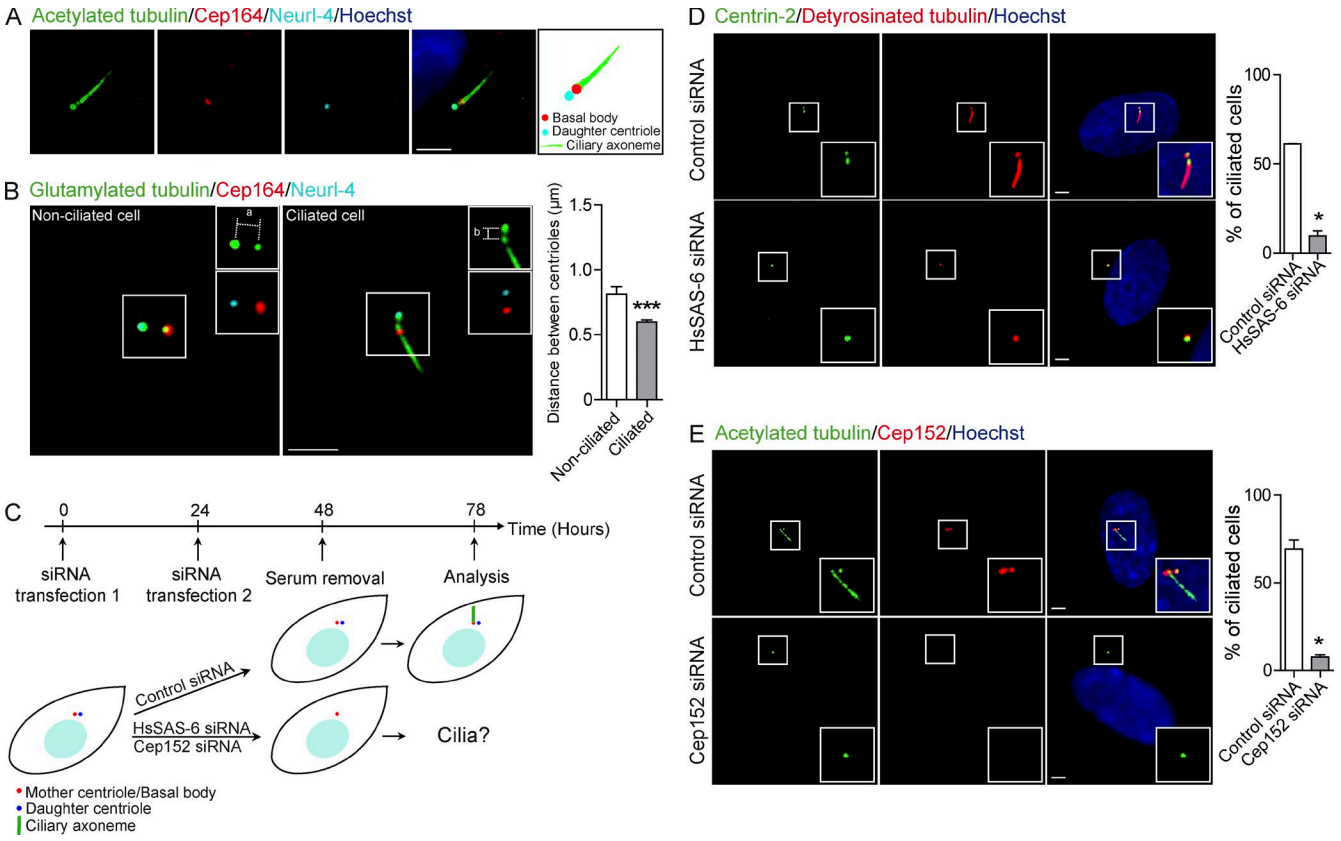

Figure 1. **Monocentriolar cells do not form primary cilia.** (A) The daughter centriole is in close proximity to the basal body in ciliated cells. The ciliary axoneme and the basal body were detected with antibodies to acetylated tubulin (green). The mother centriole/basal body and the daughter centriole were marked with antibodies to Cep164 (red) and Neurl-4 (cyan), respectively. The cartoon shows a projection of the merged image to illustrate each component of the cilium. (B) Comparison of the distance between mother and daughter centriole in nonciliated and ciliated cells. Nonciliated cells were grown in serum-rich medium, whereas ciliated cells were serum-starved for 30 h. Centrioles were labeled with antibodies to glutamylated tubulin (green), Cep164 (red), and Neurl-4 (cyan). The center of each centriole, marked with antibodies to glutamylated tubulin, was used as a reference for distance measurements between the centrioles (line a, nonciliated cell; line b, ciliated cell). The graph shows the mean distance between centrioles in nonciliated and ciliated cells. Error bars denote SEM. A total of 136 cells in three independent experiments were analyzed (***, $P < 0.001$). (C) The experimental procedure used to generate monocentriolar cells. Control cells contained two centrioles after passage through mitosis, but HsSAS-6– or Cep152-depleted cells only had a single centriole. (D) Serum-starved monocentriolar HsSAS-6–depleted cells do not form primary cilia. Centrioles and the axoneme were detected with antibodies to centrin-2 (green) and detyrosinated tubulin (red), respectively. The graph shows the mean percentage of ciliated cells from a total of 466 control and 554 monocentriolar HsSAS-6 knockdown cells ± SEM ($n = 3$; *, $P \leq 0.05$). (E) Serum-starved, monocentriolar Cep152-depleted cells do not form cilia. The same experimental approach as described in C was used. The ciliary axoneme and centrioles were labeled with antibodies to acetylated tubulin (green). Staining with Cep152-specific antibodies (red) confirmed effective knockdown. DNA was stained with Hoechst 33342. Bars, 2 µm. The graph shows the mean percentage of ciliation ± SEM from a total of 309 control and 141 monocentriolar knockdown cells ($n = 3$; *, $P \leq 0.05$).

proliferated normally and did not display increased p53 levels (Fig. S1, E and F, top). In addition, p53 depletion with a validated shRNA (Kim et al., 2007; Fig. S1 F, bottom) did not correct the cilia defects of monocentriolar cells (Fig. S1 G). Furthermore, serum-starved HsSAS-6–depleted cells did not stain with the proliferation marker Ki-67, indicating that they had exited the cell cycle and reached the nonproliferating G0 phase (Fig. S1 H). Finally, there was a significant increase in the percentage of ciliated cells when we subjected cells in serum-rich medium to thymidine-induced arrest at the G1/S transition (Fig. S1 I), suggesting that a G1 arrest may not prevent ciliogenesis. These experiments suggest that the lack of cilia from monocentriolar cells is not caused by a defect in cell cycle progression but may be caused by the absence of the daughter centriole.

Proximity between mother and daughter centrioles is required for ciliogenesis

We next examined if the proximity between the two centrioles is important for ciliogenesis by depleting the centriolar linker protein LRRC45 (Fig. 2 A). After 48 h, 6% of control cells showed separated centrioles, but the typical split centriole phenotype was observed in 24% of LRRC45-depleted cells (Fig. 2, B and C), which is similar to a published study (He et al., 2013). Loss of centriole cohesion in these cells was confirmed by staining for the centriole linker protein C-Nap1, which revealed two separate dots in the absence of LRRC45 compared with a single dot in control cells (Fig. S2 A). Control and LRRC45-depleted cells were then serum-starved for 30 h and fixed to determine the percentage of ciliated cells (Figs. 2 A and S2 B). Only 13% of LRRC45-depleted cells with separated centrioles displayed primary cilia, compared with 81.55% of LRRC45-depleted cells with adjacent centrioles and 83% of control cells (Fig. 2 C). As seen for HsSAS-6–depleted cells, this ciliogenesis defect was not caused by the activation of the centrosome integrity checkpoint (Fig. S2, C and D). In addition, lack of Ki-67 staining showed that LRRC45-depleted cells had exited the cell cycle and entered into the G0 phase (Fig. S2 E), which is consistent with the normal growth behavior reported

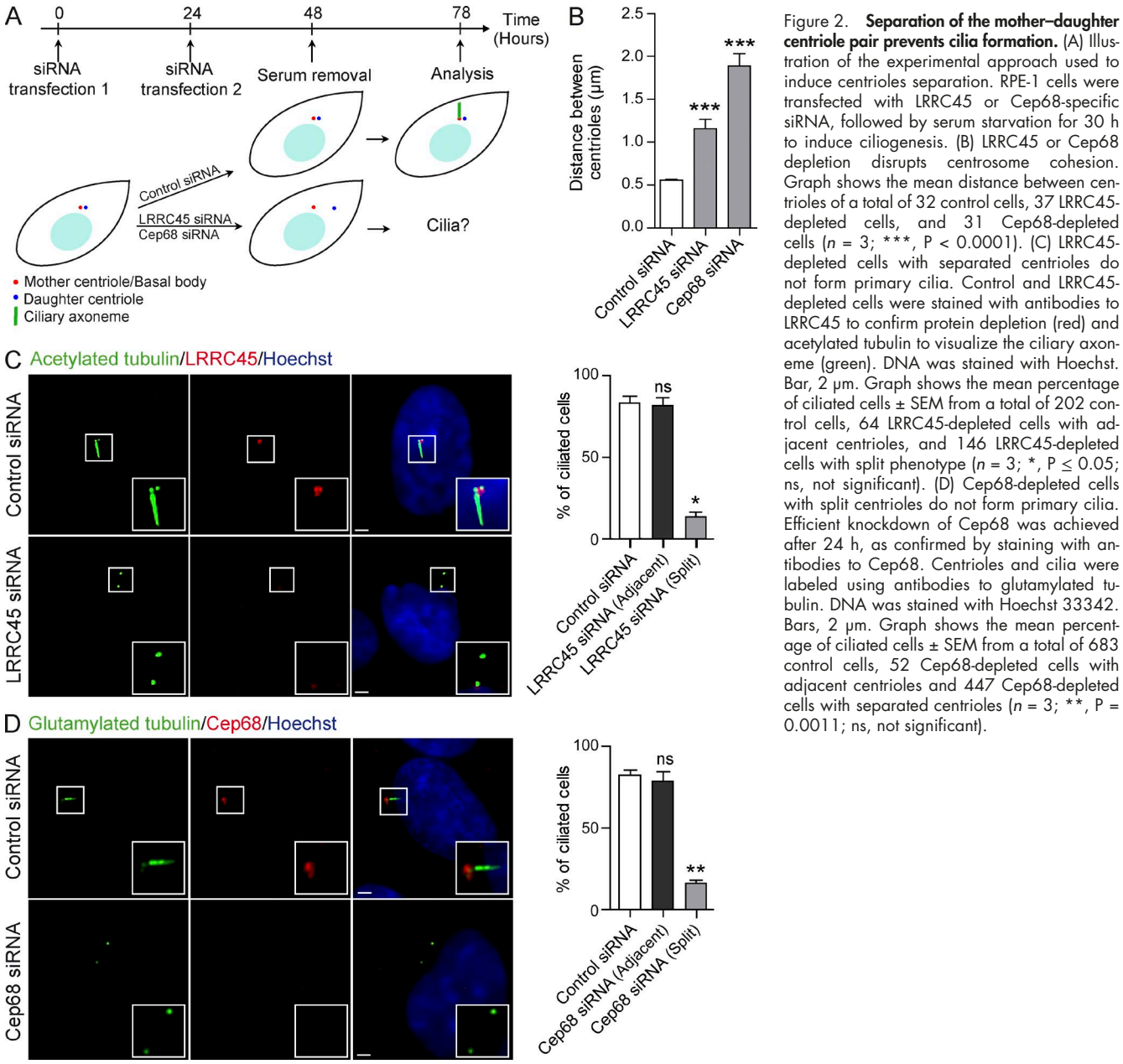

Figure 2. **Separation of the mother–daughter centriole pair prevents cilia formation.** (A) Illustration of the experimental approach used to induce centrioles separation. RPE-1 cells were transfected with LRRC45 or Cep68-specific siRNA, followed by serum starvation for 30 h to induce ciliogenesis. (B) LRRC45 or Cep68 depletion disrupts centrosome cohesion. Graph shows the mean distance between centrioles of a total of 32 control cells, 37 LRRC45-depleted cells, and 31 Cep68-depleted cells (n = 3; ***, P < 0.0001). (C) LRRC45-depleted cells with separated centrioles do not form primary cilia. Control and LRRC45-depleted cells were stained with antibodies to LRRC45 to confirm protein depletion (red) and acetylated tubulin to visualize the ciliary axoneme (green). DNA was stained with Hoechst. Bar, 2 µm. Graph shows the mean percentage of ciliated cells ± SEM from a total of 202 control cells, 64 LRRC45-depleted cells with adjacent centrioles, and 146 LRRC45-depleted cells with split phenotype (n = 3; *, P ≤ 0.05; ns, not significant). (D) Cep68-depleted cells with split centrioles do not form primary cilia. Efficient knockdown of Cep68 was achieved after 24 h, as confirmed by staining with antibodies to Cep68. Centrioles and cilia were labeled using antibodies to glutamylated tubulin. DNA was stained with Hoechst 33342. Bars, 2 µm. Graph shows the mean percentage of ciliated cells ± SEM from a total of 683 control cells, 52 Cep68-depleted cells with adjacent centrioles and 447 Cep68-depleted cells with separated centrioles (n = 3; **, P = 0.0011; ns, not significant).

for these cells (He et al., 2013). We conclude that proximity between mother and daughter centrioles is crucial for ciliogenesis. This idea was further supported by our finding that cells with split centrioles caused by depletion of another centriole cohesion factor, Cep68 (Graser et al., 2007b), were unable to form primary cilia (Figs. 2 D and S2 D).

A daughter centriole adjacent to the mother is necessary for CP110 removal

To understand the molecular basis of this ciliogenesis defect, we examined the effects of daughter centriole manipulations on the protein composition of the basal body by immunofluorescence (IF) microscopy. Our experimental conditions produced no apparent defect in the basal body association of the two distal appendage proteins Cep164 and Cep123, which are both required for ciliogenesis (Graser et al., 2007a; Sillibourne et al., 2013; Fig. S3, A and B). Also, the localization of ODF2, another mother centriole protein (Ishikawa et al., 2005), was unaffected (Fig. S3 C). Similarly, TMEM67, a component of the transition zone, localized to the basal body in cells with manipulated daughter centrioles (Fig. S3 D). Furthermore, IFT88, a subunit of the IFT-B complex, was normally recruited to the basal body in daughter centriole–manipulated cells (Fig. S3 E). These observations suggest that the recruitment of these specific ciliogenesis regulators to the basal body is unaffected by our experimental conditions.

We also monitored the distribution of the negative ciliogenesis regulator CP110 in HsSAS-6– and LRRC45-depleted cells. In 94% of control cells, CP110 was efficiently removed from the mother centriole so that it was only detected at the daughter centriole (Fig. 3 A). In contrast, 81% of HsSAS-6–depleted cells with only a mother centriole and 78% of LRRC45-depleted cells with separated centrioles displayed CP110 at the mother centriole (Fig. 3 A), which is indicative of CP110 stabilization at this location. Consistent with these observations, increased CP110 protein levels were detected

in total lysates from cells depleted of HsSAS-6 and LRRC45 (Fig. 3 B). CP110 stabilization was also seen in cells depleted of Cep152 or Cep68 (unpublished data). As codepletion of CP110 restored primary cilia formation in cells with daughter centriole manipulations (Fig. 3, C and D; and Fig. S3 F), we conclude that the absence of cilia in these cells is caused by CP110 stabilization at the mother centriole.

Daughter centriole manipulations affect the ubiquitin ligase cofactor Neurl-4

We next tested if daughter centriole manipulations affect CP110 regulation by altering the machinery known to control CP110 protein levels. We first examined the centrosome-associated ubiquitin ligase HERC2, which has been linked to CP110 degradation (D'Angiolella et al., 2010; Al-Hakim et al., 2012). This protein localized normally to the centrosome in cells with manipulated daughter centrioles (Fig. 4 A). We also examined the protein kinase TTBK2, whose recruitment to the mother centriole early during ciliogenesis is required for CP110 removal and cilia formation (Goetz et al., 2012). Although TTBK2 was detected at the centrosome, its levels were reduced in 49% of HsSAS-6–depleted, monocentriolar cells compared with 13% of control cells (Fig. 4, B and C). LRRC45-depleted cells displayed a similar reduction in TTBK2 recruitment (Fig. 4, B and C). Interestingly, the association of IFT88 with the basal body, which depends on centrosomal TTBK2, was normal in both HsSAS-6– and LRRC45-depleted cells (Fig. S3 E; Goetz et al., 2012). This result suggests that TTBK2, even at reduced levels, may be functional at the basal body. It is therefore unlikely that CP110 stabilization at the mother centriole of cells with manipulated daughter centrioles is caused by a partial defect in TTBK2 recruitment. Finally, we examined the ubiquitin ligase cofactor Neurl-4, which is critical for CP110 degradation (Li et al., 2012). Neurl-4 was completely absent from the single centriole in ∼85% of HsSAS-6–depleted monocentriolar cells (Fig. 4, D [top and middle] and E). In contrast, it was present at the daughter centriole in ∼90% of LRRC45-depleted cells (Fig. 4, D [top and bottom] and E), although its proximity to the mother centriole was clearly abolished in these cells. Our results suggest that daughter centriole manipulations disrupt the spatial relationship between Neurl-4 and the mother centriole, which may be necessary for proper CP110 regulation and ciliogenesis.

Neurl-4 is a novel regulator of ciliogenesis

We investigated if Neurl-4 is important for ciliogenesis. Similar to the procedure described in Fig. 1 C, we transfected cells for 48 h with siRNA against Neurl-4 and then serum-starved them for 30 h. With this procedure, we obtained 23% of cells with significantly lower Neurl-4 levels at the daughter centriole (Fig. S4), and these cells were unable to form primary cilia (Fig. 5 A). Depletion of Neurl-4 resulted in ectopic CP110 foci in the perinuclear region and increased CP110 levels in total cell lysates (Fig. 5, A and B), confirming the reported requirement for Neurl-4 in CP110 degradation (Li et al., 2012). We also found that overexpression of mCherry-tagged Neurl-4 for 30 h in serum-rich medium promoted CP110 down-regulation (Fig. 5 C), although ciliogenesis was not enhanced in this experiment (not depicted). Altogether, these results confirm the contribution of Neurl-4 to CP110 regulation and identify a novel role of this cofactor protein in primary ciliogenesis.

Neurl-4 is sufficient to rescue cilia defects in monocentriolar cells

To test if the lack of centrosomal Neurl-4 is responsible for the ciliogenesis defects in monocentriolar cells, we performed a rescue experiment in which we targeted Neurl-4 to the centrosome. mCherry-Neurl-4 by itself did not localize to the mother centriole in monocentriolar cells and was unable to restore ciliogenesis. We therefore targeted mCherry-Neurl-4, or mCherry as a negative control, to the centrosome through the PACT (pericentrin/AKAP450 centrosomal targeting) domain, a known centrosomal targeting motif (Gillingham and Munro, 2000; Fig. 6 A). 30 h after transfection and serum starvation, mCherry-PACT and mCherry-PACT-Neurl-4 were observed at the centrosome at similar levels in control and HsSAS-6–depleted cells (Fig. 6, B and C). Cells were then analyzed for the presence of cilia (Fig. 6, B and D). 46% of monocentriolar HsSAS-6–depleted cells expressing mCherry-PACT-Neurl-4 displayed primary cilia compared with 23% of control cells expressing mCherry-PACT (Fig. 6 D). These cells also had reduced CP110 levels (Fig. 6, B and E). We conclude that centrosomally targeted Neurl-4 is sufficient to partially rescue the cilia defects of monocentriolar cells. Interestingly, restored cilia, which were similar in length as control cilia, were composed of only a basal body and a ciliary axoneme but clearly lacked the daughter centriole (Fig. 6 B, bottom).

Transient translocation of Neurl-4 to the mother centriole precedes axoneme elongation

As our studies identified a critical role for Neurl-4 in ciliogenesis, we monitored the behavior of this protein during early stages of cilia formation. We serum-starved wild-type RPE-1 cells and observed Neurl-4 localization in a time course experiment at 0, 6, 12, and 30 h after serum withdrawal (Fig. 7 A, top). In proliferating cells (0-h time point) Neurl-4 only associated with the daughter centriole. However, after 6 h of serum starvation, a small fraction of Neurl-4 was detected at the mother centriole, forming a continuous, thin connection between the two Neurl-4 dots (Fig. 7 A, top). 12 h after serum removal, which is when axoneme extension begins, Neurl-4 was still at the mother centriole. However, at 30 h after serum starvation, axoneme formation was complete and Neurl-4 was no longer detectable at the mother centriole (Fig. 7 A, top). Similar observations were made in human foreskin fibroblast (HFF) cells (Fig. S5), confirming the interesting behavior of this protein in a primary human cell line. This transient Neurl-4 translocation to the mother centriole was not detected in LRRC45-depleted cells, in which the protein remained on the daughter centriole at all time points (Fig. 7 A, bottom). These results suggest that the transient exchange of Neurl-4 between the two centrioles is facilitated by their physical proximity.

Our results are consistent with a model in which the daughter centriole is critical for the regulation of Neurl-4 localization within the centrosome. In nonciliated, dividing (Fig. 7 B, 1) and fully ciliated quiescent cells (3), Neurl-4 localizes exclusively to the daughter centriole. However, early in ciliogenesis, before axoneme extension (Fig. 7 B, 2), a small fraction of this protein transiently translocates from the daughter centriole to the mother in a process that requires proximity between the two centrioles. If Neurl-4 cannot reach the mother centriole, CP110 removal does not occur, preventing cilia formation. We speculate that at the mother centriole, Neurl-4 interacts with additional factors, such

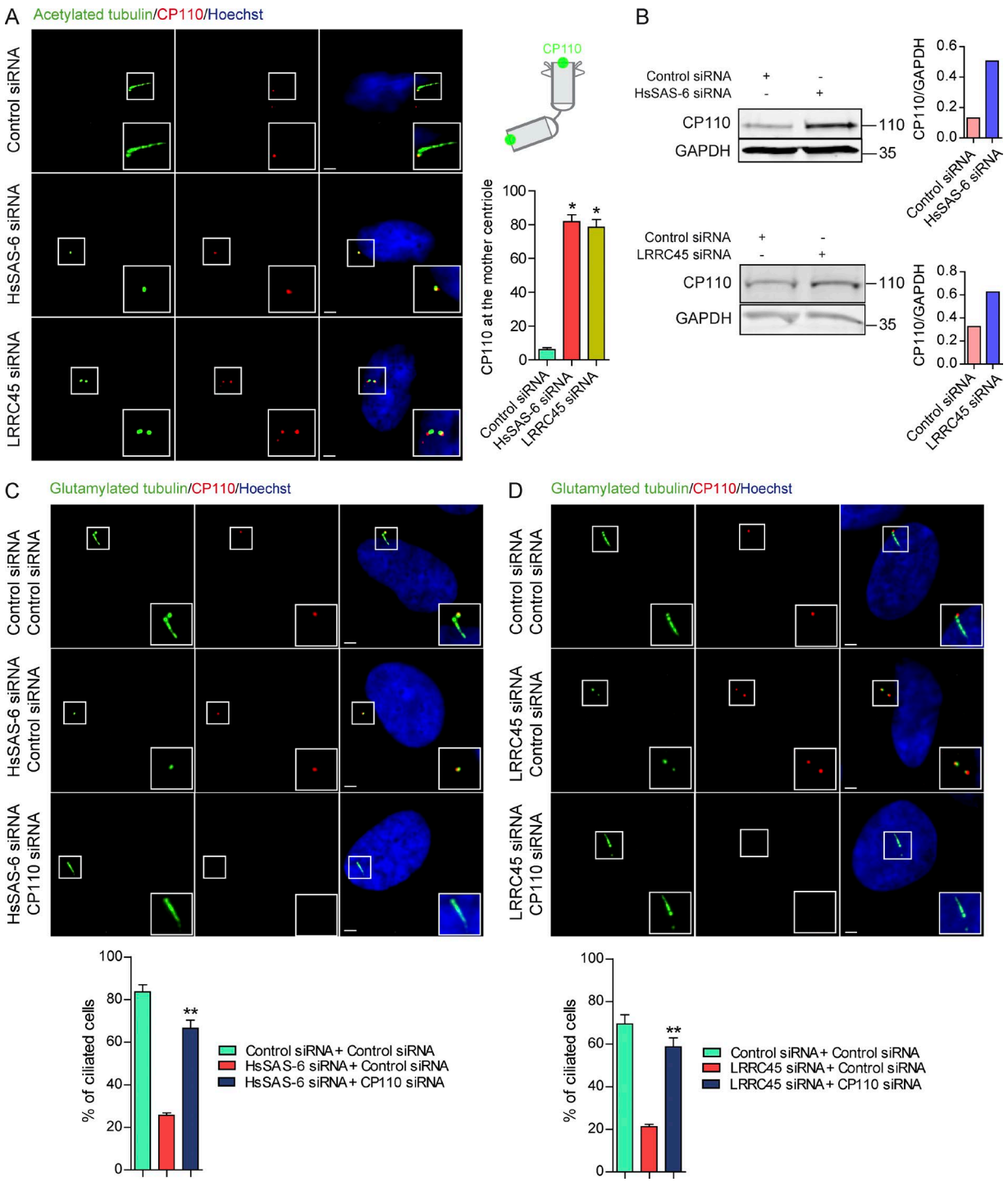

Figure 3. **Ciliogenesis defects in cells with manipulated daughter centrioles are caused by CP110 stabilization at the mother centriole.** (A) The negative ciliogenesis regulator CP110 is not removed from the mother centriole of HsSAS-6– or LRRC45-depleted cells. The cartoon shows the localization of this protein in cycling cells. CP110 was visualized by IF microscopy using CP110-specific antibodies in these cells. Bars, 2 µm. Graph shows the mean percentage of cells with CP110 at the mother centriole ± SEM. A total of 111 control, 198 monocentriolar and 141 LRRC45-depleted cells was quantified from 3 independent experiments (*, $P \leq 0.05$). (B) Representative Western blots showing CP110 levels in whole-cell extracts of control and HsSAS-6–depleted cells (top) or control and LRRC45-depleted cells (bottom) at 78 h after siRNA transfection. GAPDH served as loading control to normalize the CP110 signal (shown in arbitrary units) in each blot. Quantifications of these Western blots are shown. (C) CP110 depletion restores cilia formation in monocentriolar cells after CP110 depletion. Cells were stained with antibodies to glutamylated tubulin (green) and CP110 (red), DNA was detected with the DNA dye Hoechst 33342. Bars, 2 µm. The graph shows the mean percentage of ciliated cells ± SEM for cells that were either transfected twice with control siRNA ($n = 150$ cells), once with HsSAS-6–specific siRNA, then with control siRNA ($n = 109$ cells), or once with HsSAS-6 siRNA, then with CP110-specific siRNA ($n = 137$ cells; $n = 3$; **, $P \leq 0.004$). (D) CP110 depletion is sufficient to rescue ciliogenesis defects in LRRC45-depleted cells. Same experiment as C, except for the depletion of LRRC45 instead of HsSAS-6: control siRNA/control siRNA ($n = 255$ cells), LRRC45 siRNA/control siRNA ($n = 278$ cells), and LRRC45 siRNA/CP110 siRNA ($n = 122$ cells; $n = 3$; **, $P = 0.0022$). DNA was stained with Hoechst. Bars, 2 µm.

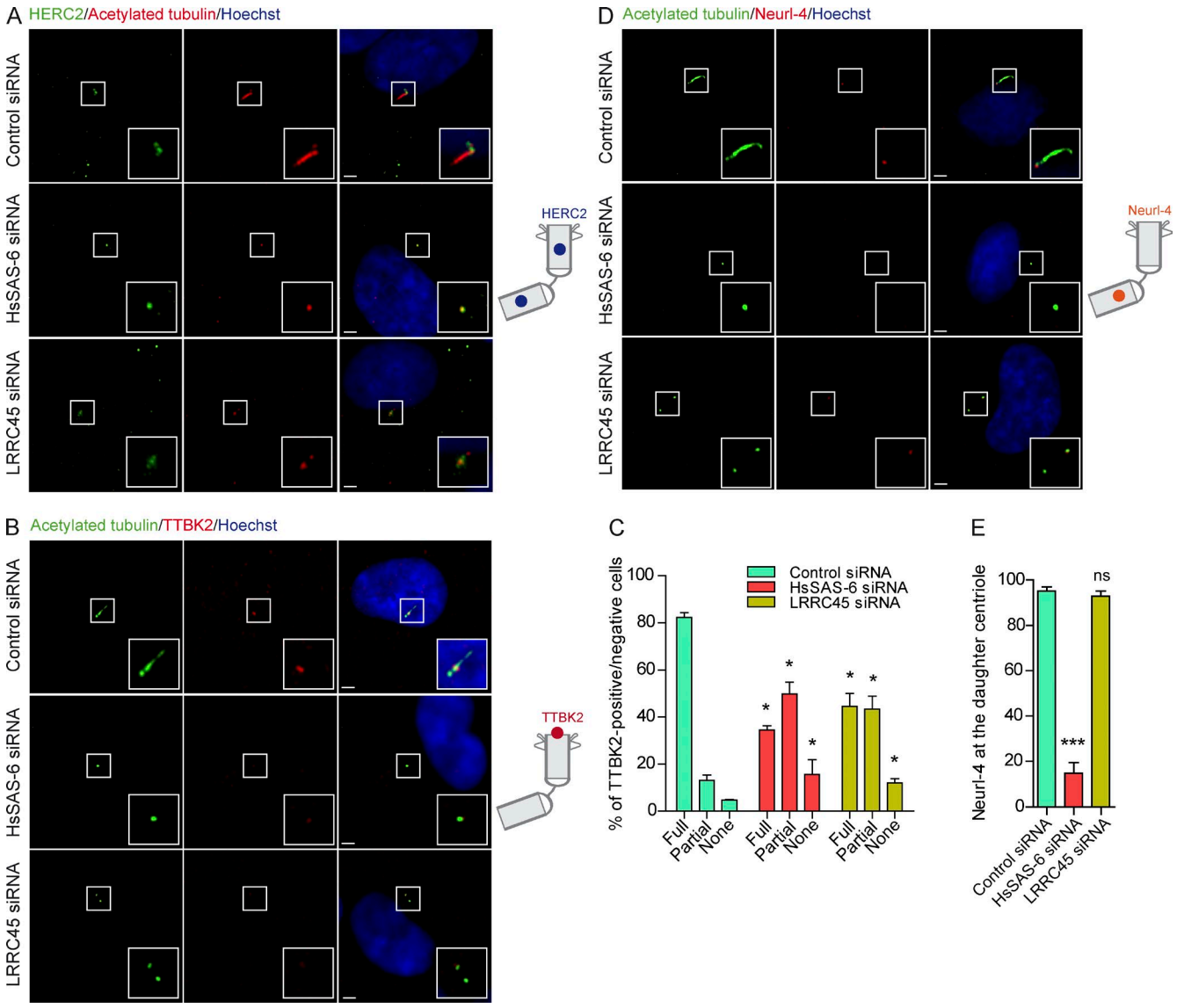

Figure 4. **Daughter centriole manipulations affect TTBK2 and Neurl-4 localization.** The association of selected CP110 regulators with the basal body was analyzed in control and monocentriolar HsSAS-6–depleted cells as well as LRRC45-depleted cells with separated centrioles. All panels show merged images with DNA stained with Hoechst 33342. Bars, 2 µm. (A) Ciliary axoneme and centrioles were labeled with antibodies to acetylated tubulin (red) and HERC2 (green). (B) Acetylated tubulin and TTBK2 are shown in green or red, respectively. (C) The graph shows the quantification of TTBK2 levels (full, partial, or none) at the basal body. The percentage of cells in each category is shown for a total of 191 control cells, 56 HsSAS-6–depleted cells, and 75 LRRC45-depleted cells (n = 3; *, $P \leq 0.05$). The signal for acetylated tubulin was used for normalization. (D) Acetylated tubulin and Neurl-4 are shown in green or red, respectively. (E) Graph shows the mean percentage of cells with Neurl-4 at the daughter centriole from 145 control cells, 73 HsSAS-6–depleted cells, and 77 LRRC45-depleted cells (n = 3; ***, $P < 0.0001$; ns, not significant).

as an E3 ligase, that facilitate CP110 removal and ciliogenesis (Fig. 7 B). In an alternative model (Fig. 7 B, 4), Neurl-4 is directly recruited to the mother centriole to control local CP110 levels.

Discussion

In this study, we provide support for a novel role of the daughter centriole in primary cilia formation. Cells in which the daughter centriole was either absent (HsSAS-6 or Cep152 depletion) or separated from its mother (LRRC45 or Cep68 depletion) were unable to form primary cilia. This ciliogenesis defect was due to CP110 stabilization at the mother centriole and was corrected by CP110 depletion. We also show that Neurl-4 is necessary for ciliogenesis and that this ubiquitin ligase cofactor transiently associates with the mother centriole early during ciliogenesis. We integrate our findings into the bridge model, in which the daughter centriole, adjacent to its mother, facilitates Neurl-4 translocation to the mother centriole, which may promote the localized CP110 removal that is necessary for ciliogenesis. Our model is consistent with the reported role of the centriole cohesion factor rootletin in ciliogenesis (Conroy et al., 2012) and provides a functional explanation for the presence of the daughter centriole next to the mother during ciliogenesis. However, our data can also be explained by an alternative model (recruitment model), in which LRRC45 and Cep68 control ciliogenesis by directly recruiting Neurl-4 or other CP110 regulatory factors to the mother centriole early during ciliogenesis. It is possible

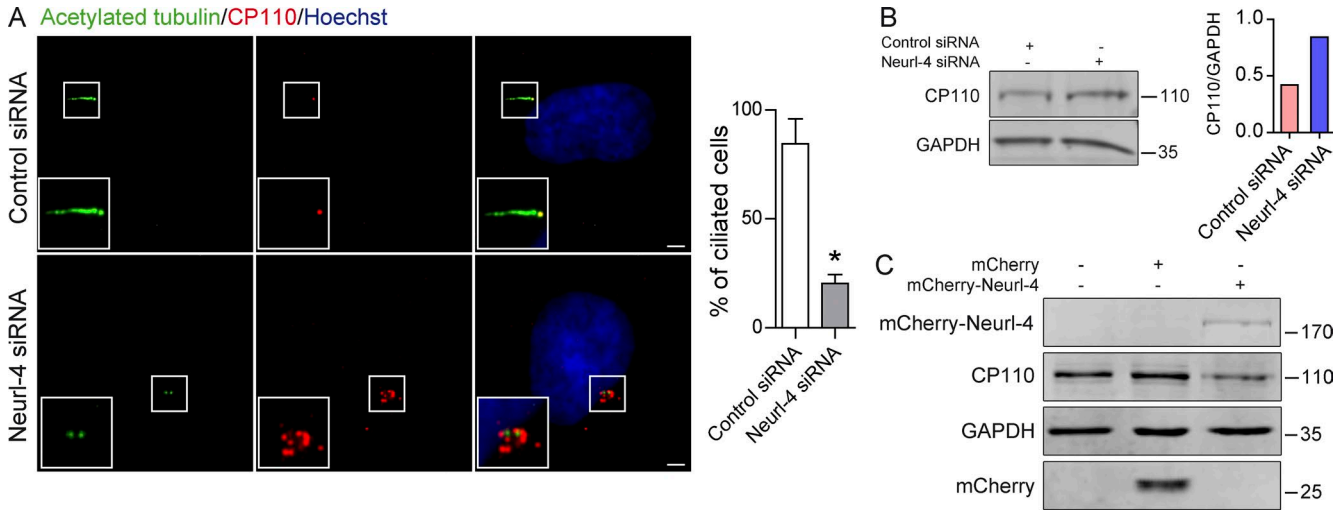

Figure 5. **Neurl-4 controls CP110 levels and is required for ciliogenesis.** (A) Effects of Neurl-4 depletion on cilia formation. Neurl-4 depletion was performed using the same experimental protocol previously described in Fig. 1 C. Centrioles and cilia were stained with antibodies to acetylated tubulin (green) and CP110 (red). Merged images with DNA stained with Hoechst are also shown. Bars, 2 µm. Graph shows the percentage of ciliated cells from a total of 244 control cells and 181 Neurl-4–depleted cells (n = 3; *, $P \leq 0.05$). (B) Neurl-4 depletion leads to increased CP110 levels. CP110 levels were monitored in total cell lysates at 78 h after siRNA transfection from control and Neurl-4–depleted cells using Western blot analysis. GAPDH served as loading control to normalize the CP110 signal (shown in arbitrary units) in each blot. A quantification of this Western blot is shown. (C) Neurl-4 overexpression destabilizes CP110 in cycling cells. The constructs pmCherry and pmCherry-Neurl-4 were transfected into proliferating RPE-1 cells and expressed for 30 h. Representative Western blots showing CP110 levels in nontransfected control cells and in cells expressing mCherry- and mCherry-Neurl-4. The levels of exogenously expressed proteins were monitored with antibodies to mCherry. GAPDH served as a loading control.

that LRRC45 and Cep68 form a complex at the proximal end of the mother centriole, providing a docking site for other proteins. Such a function of these centriole cohesion factors may be independent of their normal role in centriole cohesion and could be disrupted in monocentriolar cells.

Neurl-4 is a central component of our model. This protein belongs to the family of neuralized-like proteins and was shown to associate with the daughter centriole (Li et al., 2012). Another study detected this protein predominantly at the mother centriole (Al-Hakim et al., 2012), but we confirmed the specificity of its daughter centriole localization through depletion and overexpression experiments (Fig. S4 and not depicted). Interestingly, we detected a small fraction of Neurl-4 at the mother centriole early during ciliogenesis in two different cell lines. This association was transient and not observed in cells that were either dividing or displaying a fully formed axoneme. The Neurl-4 population at the mother centriole is likely to originate from the daughter because transient Neurl-4 recruitment to the mother did not occur in cells with split centrioles. In addition, there appeared to be a continuous thread of Neurl-4 between the two centrioles early during ciliogenesis. However, we cannot exclude the possibility that Neurl-4 is recruited to the mother centriole from the cytosol. At this point, we do not know how Neurl-4 moves between centrioles and if other proteins display a similar dynamic behavior.

Our main model is in conflict with recent reports on C-Nap1. CRISPR/Cas9 or ZNF-mediated knockout of this centriole cohesion factor produced RPE-1 cells that had split centrioles but no defect in cilia formation or length (Panic et al., 2015; Mazo et al., 2016; Flanagan et al., 2017). Furthermore, previously observed ciliogenesis defects in cells depleted of C-Nap1 by siRNA were found to be due to off-target effects (Conroy et al., 2012; Sillibourne et al., 2013; Flanagan et al., 2017). There are two major differences between these reports and our study. (1) They used CRISPR/Cas9 or ZNF strategies, which generate permanent knockout clones that were selected for their ability to survive. RNAi, in contrast, generates transient and often partial protein knockdown that may be able to reveal a specific phenotype (Boettcher and McManus, 2015). CRISPR/Cas9 and RNAi have produced contradicting results for other centrosomal proteins. For example, for the subdistal appendage protein ODF2, CRISPR-mediated knockout cells had normal cilia (Mazo et al., 2016), whereas RNAi experiments revealed significant ciliogenesis defects (Kuhns et al., 2013). Opposite results were also reported for microtubule organization by subdistal appendage proteins (Mazo et al., 2016). (2) We observed ciliogenesis defects in the absence of two cohesion factors LRRC45 and Cep68, which both form fibers between the two centrioles (Graser et al., 2007b; He et al., 2013). C-Nap1, in contrast, associates with the proximal end of mother and daughter centrioles and forms docking sites for other cohesion factors, including Cep68 and LRRC45 (He et al., 2013; Fang et al., 2014). It is not known how permanent C-Nap1 loss affects Cep68 and LRRC45 localization and function. Overall, our results call for a detailed analysis of the link between centriole cohesion and ciliogenesis, comparing RNAi and knockout methods for the different centriole cohesion factors.

We propose that Neurl-4–dependent CP110 degradation is restricted to the mother centriole. However, the simple presence of Neurl-4 and CP110 at the same centriole appears insufficient for CP110 degradation because both proteins localize to the daughter centriole, but CP110 is not degraded. Although it is not known when and where Neurl-4 and CP110 interact, our data suggest that an additional factor may be required for Neurl-4–mediated CP110 degradation at a specific site. Similarly, cyclin F and CP110 colocalize during the cell cycle, but their actual interaction is only detected in G2, followed by CP110 degradation at the M/G1 transition (D'Angiolella et al., 2010). As Neurl-4 seems to act as an ubiquitin ligase cofactor, it is possible that the younger centriole lacks the ubiquitin ligase

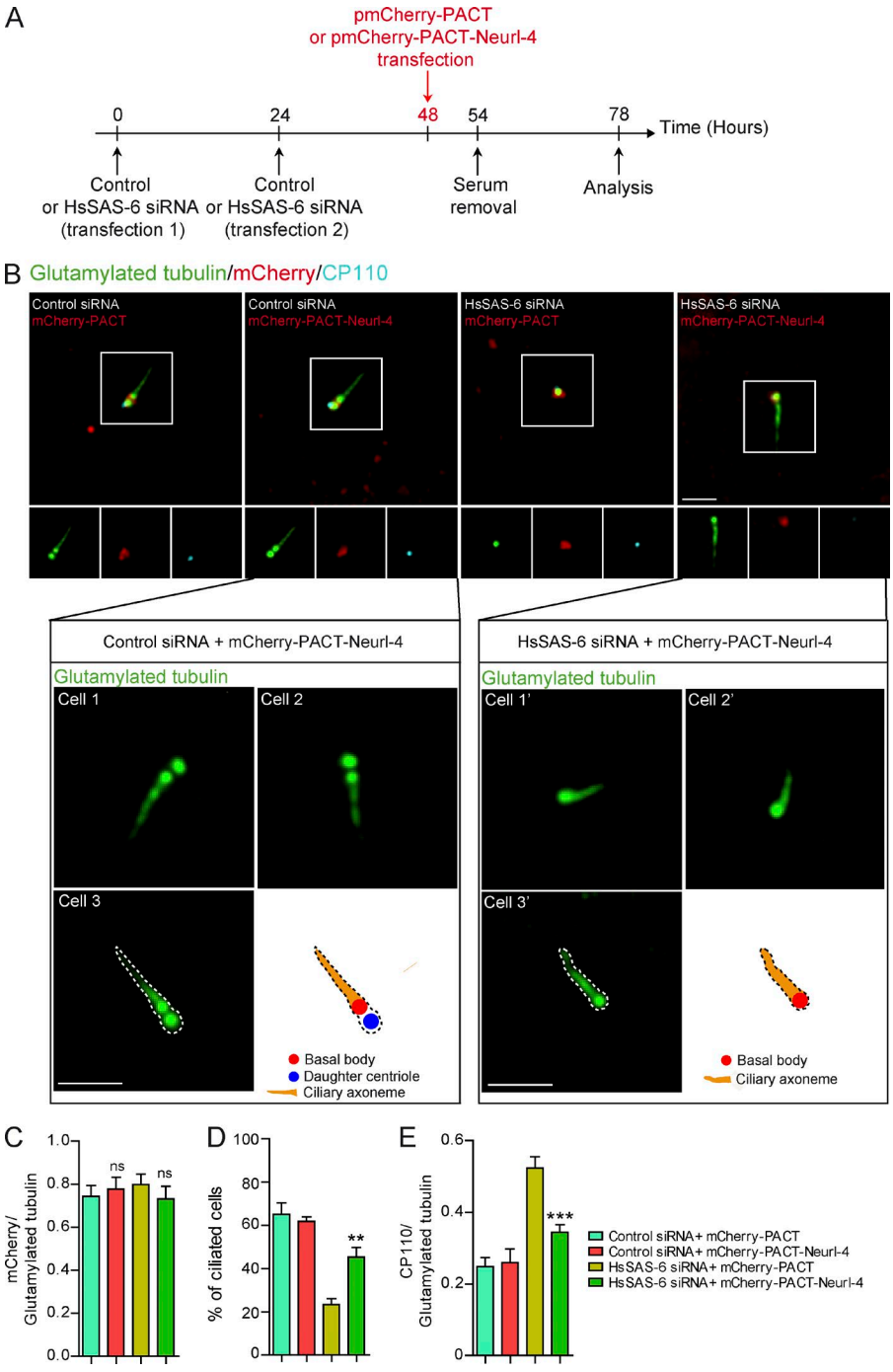

Figure 6. **Targeting Neurl-4 to the mother centriole is sufficient to rescue ciliogenesis defect of monocentriolar cells.** (A) Experimental procedure of the rescue experiment. Control and monocentriolar RPE-1 cells were transfected with pmCherry-PACT or pmCherry-PACT-Neurl-4. Cells were deprived of serum for 24 h and examined for their ability to form primary cilia. (B) Representative IF images of control and HsSAS-6–depleted cells expressing either pmCherry-PACT or pmCherry-PACT-Neurl-4 (top). Ciliary axonemes and centrioles were stained with antibodies to glutamylated tubulin (green), whereas CP110 was detected with specific antibodies (cyan). mCherry-tagged proteins were detected with antibodies to mCherry (red). Comparison of cilia emanating from a basal body with or without daughter centriole (bottom). Three cells (cells 1–3), in which cilia are stained with antibodies to glutamylated tubulin, are shown for each condition. Cartoons of the cilia of cell 3 and cell 3′ are also shown. Bars, 2 µm. (C) The intensity of mCherry at the centrosome of at least 10 cells was quantified for each condition (ns, not significant). (D) The graph shows the mean percentage of ciliated cells in the rescue assay. For each condition ∼100 cells were quantified from three independent experiments (n = 475 cells; **, $P \leq 0.01$). (E) The graph shows the mean intensity of CP110 at the mother centriole, which was normalized to glutamylated tubulin (shown as arbitrary units; n = 155 cells; ***, $P \leq 0.0001$).

that mediates CP110 degradation or contains an inhibitor of CP110 degradation. The mother centriole, in contrast, may actively promote the association between Neurl-4, CP110, and the ubiquitin ligase to enhance CP110 degradation. The identity of this ubiquitin ligase is not known, although the established interaction of Neurl-4 with HERC2 makes this protein a possible candidate (Al-Hakim et al., 2012; Martínez-Noël et al., 2012).

The observed ciliogenesis defects are unlikely to be caused by activation of the p53-dependent centrosome integrity checkpoint in G1 (Mikule et al., 2007; Wong et al., 2015). This arrest was, for example, seen after centrosome fragmentation due to the depletion of certain centrosomal components, or inactivation of Plk4 using the pharmacological inhibitor centrinone or CRISPR/Cas9 (Mikule et al., 2007; Wong et al., 2015; Fong et al., 2016; Lambrus et al., 2016). However, our experimental conditions did not induce a G1 arrest because (1) the growth rate of HsSAS-6–depleted cells was comparable to that of control cells, (2) p53 levels were unaffected by HsSAS-6 or LRRC45 depletion, and (3) the ciliogenesis defects were not corrected by p53 depletion. Moreover, we show that induction of a G1/S cell cycle arrest did not disrupt but rather promoted ciliogenesis, which further argues against a G1 arrest as an explanation for the observed ciliogenesis defects. These results indicate that depletion of centrosomal proteins, at least at early time points and in combination with serum starvation, does not activate the centrosome integrity checkpoint or induce cell cycle arrest.

Several studies have linked primary cilia loss to cancer development and progression (Gradilone et al., 2013; Hassounah

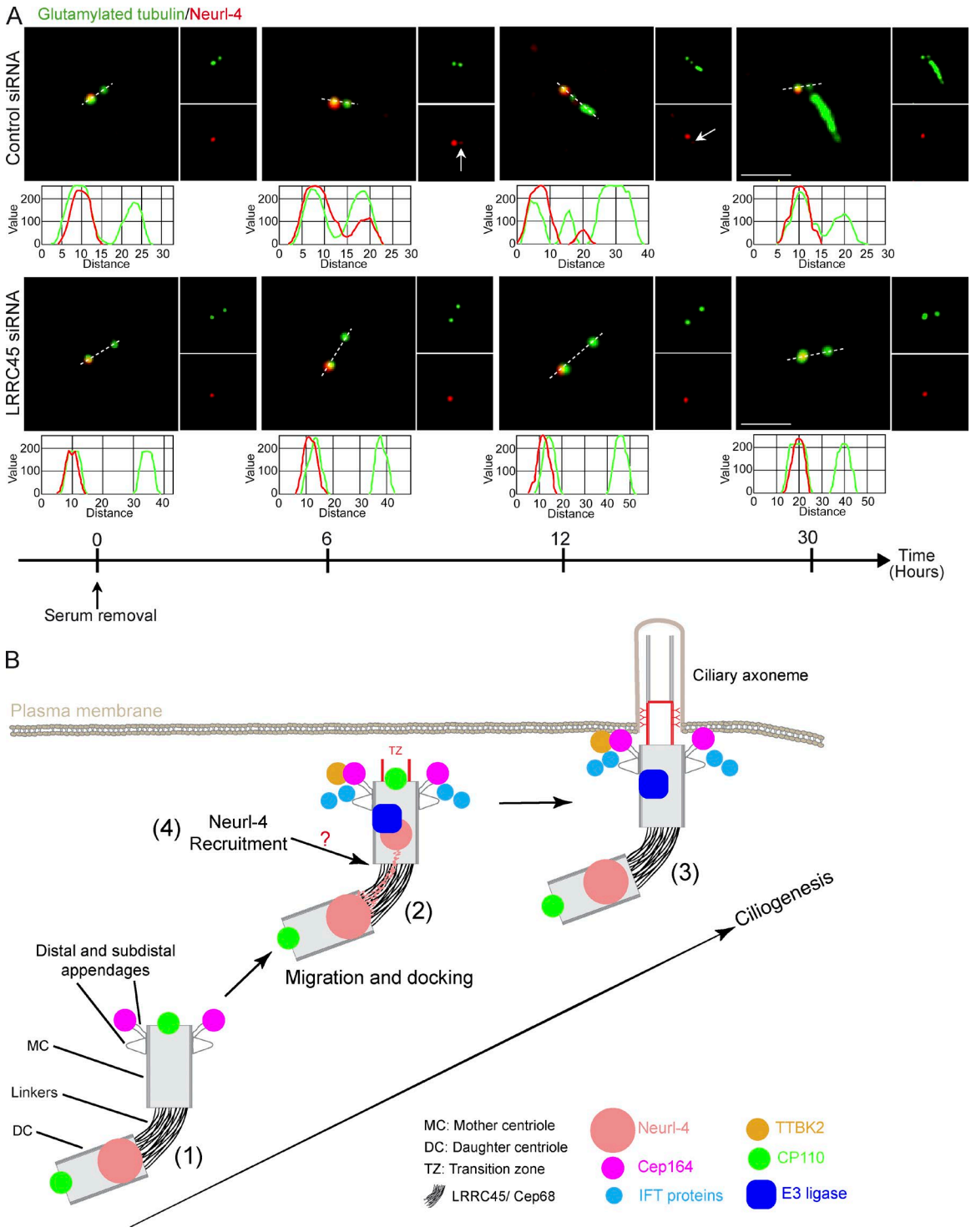

Figure 7. **Transient translocation of Neurl-4 from the daughter to the mother centriole depends on proximity between the two centrioles.** (A) Observation of Neurl-4 localization (red) in response to serum removal in control and LRRC45-depleted cells. Centrioles and cilia were labeled with glutamylated tubulin (green). Fluorescence spectra plots of Neurl-4 and glutamylated tubulin (corresponding to the white dashed lines) are shown underneath images (vertical axis: gray level; horizontal axis: distance in pixels). Representative images of two independent experiments, with data collection from two different slides for each experiment. Bars, 2 µm. (B) Model for daughter centriole–mediated regulation of ciliogenesis (1–3). Bridge model: Neurl-4 associates with the daughter centriole in cycling cells (1), but when cilia formation is induced (2), it transiently moves to the mother centriole in a process that depends on proximity between the two centrioles. (3) At the mother centriole, Neurl-4 then may interact with other factors, such as E3 ligases to facilitate CP110 removal from the mother centriole and promotes ciliogenesis. (4) Recruitment model: LRRC45 and Cep68 control the recruitment of Neurl-4 or other CP110 regulatory factors to the mother centriole, possibly from the cytosolic pool, thereby facilitating local CP110 removal at the mother centriole.

et al., 2013; Menzl et al., 2014). For example, genes that support cilia biogenesis and function were found to be dysregulated in cancer (Shpak et al., 2014). In addition, some cancers, such as breast malignancies, display significantly fewer cilia than control tissue (Menzl et al., 2014). Interestingly, Neurl-4 is down-regulated in several tumors, including those of the prostate and kidney (Uhlén et al., 2005), which are both associated with primary cilia loss (Basten et al., 2013; Hassounah et al., 2013). Although this correlation is intriguing, additional studies are necessary to understand the role of Neurl-4 in cancer progression and cilia regulation.

Over many years, the daughter centriole has remained enigmatic because few proteins are reported to specifically associate with this younger centriole, and their function is not well understood. Our study provides first support for a role of the daughter centriole in primary cilia formation. This function depends on the position of the daughter centriole next to the mother to promote CP110 removal and conversion of the mother centriole into the basal body. In addition to providing a platform for Neurl-4 recruitment, the daughter centriole facilitates the movement of a protein between the two centrioles during ciliogenesis. Thus, our study has revealed a novel physical and functional relationship between daughter and mother centrioles.

Materials and methods

Antibodies

Antibodies and their conditions of use are detailed as follows: mouse anti–acetylated tubulin (IF: methanol or formaldehyde, 1:6,000; T6793; Sigma-Aldrich), rabbit anti–acetylated tubulin (IF: methanol, 1:200; 5335; Cell Signaling Technology); goat anti-Cep64 (IF: methanol, 1:250; sc-240226; Santa Cruz Biotechnology, Inc.), rabbit anti–Neurl-4 (IF: methanol, 1:250; gift from B. Dynlacht, NYU Cancer Institute, New York, NY; Li et al., 2012), mouse anti-Centrin2 (IF: methanol, 1:1,000; 04-1624; EMD Millipore), rabbit anti–detyrosinated tubulin (IF: methanol, 1:500; AB3201; EMD Millipore), mouse anti–polyglutamylated tubulin (IF: methanol, 1:500, GT335; AG-20B0020; AdipoGen), rabbit anti-Cep152 (IF: methanol, 1:500; A302-479A; Bethyl Laboratories, Inc.), rabbit anti-Par6G (IF: methanol, 1:500; G9547; Sigma-Aldrich), rabbit anti–Ki-67 (IF: formaldehyde, 1:2,000; Ab15580; Abcam), rabbit anti-LRRC45 (IF: methanol, 1:500; HPA024768; Sigma-Aldrich), Cep68 (IF: methanol, 1:100; A302-533A; Bethyl Laboratories, Inc.), mouse anti–C-Nap1 (IF: methanol, 1:100; 611374; BD), mouse anti-p53 (IF: methanol; 1:1,000, 2524; Cell Signaling Technology), rabbit anti-MKS3 (TMEM67; IF: methanol, 1:100; 13975-1-AP; Proteintech), rabbit anti-CP110 (IF: methanol, 1:500; WB: 1:500; 12780-1-AP; Proteintech), mouse anti–HsSAS-6 (IF: methanol, 1:400; WB: 1:500; sc-81431; Santa Cruz Biotechnology, Inc.), mouse anti-HERC2 (IF: methanol, 1:100; 612366; BD), rabbit anti–cyclin F (IF: methanol, 1:100; sc-952; Santa Cruz Biotechnology, Inc.), rabbit anti-TTBK2 (IF: formaldehyde in general tubulin buffer [GTB: 80 mM Pipes, pH 7, 1 mM $MgCl_2$, and 1 mM EGTA], 1:500; HPA018113; Sigma-Aldrich), rabbit anti-Cep123 (IF: methanol, 1:500; gift from M. Bornens, Institut Curie, Paris, France; Sillibourne et al., 2013), rabbit anti-ODF2 (IF: methanol, 1:50; HPA001874; Sigma-Aldrich), goat anti-IFT88 (IF: methanol/acetone [1:1], 1:250; Ab42497; Abcam), mouse anti-GAPDH (WB: 1:10,000; sc-47724; Santa Cruz Biotechnology, Inc.), and goat anti-mCherry (IF: methanol, 1:400; WB: 1:1,000; AB0040-200; SICGE).

Cell culture, constructs, and transient transfection

Retinal pigment epithelium (hTERT-RPE1) cells (provided by B. Dynlacht, NYU Cancer Institute, New York, NY) and HFF cell line (provided by N. Morrissette, University of California, Irvine, Irvine, CA) were grown in DMEM (Gibco) with 10% FBS (Hyclone). Cells were grown in a humidified 5% CO_2 incubator at 37°C. Human Neurl-4 cDNA (provided by B. Dynlacht; Li et al., 2012) was PCR amplified and subcloned into pmCherry-N1 (Takara Bio, Inc.) using HindIII and SalI restriction sites. PACT domain was PCR amplified from the human AKAP450 sequence (gift from M. Takahashi, Teikyo Heisel University, Nakano, Japan) and subcloned into pmCherry-N1 or pmCherry-N1-Neurl-4 using NotI and HpaI restriction sites. The sequence of each construct was confirmed by sequence analysis (Retrogen, Inc.). All constructs were transfected using X-tremeGENE 9 DNA transfection reagent (Roche) following the manufacturer's instructions. Recombinant proteins were overexpressed for 24 to 30 h.

RNAi

The following siRNAs were used in this study: Scrambled control siRNA, 5′-ACUAAACUGAGGCAAUGCC-3′; HsSAS-6, 5′-GCACGUUAAUCAGCUACAA-3′ (Leidel et al., 2005); Cep152, 5′-GCGGAUCCAACUGGAAAUCUA-3′ (Cizmecioglu et al., 2010); LRRC45, 5′-CCAACAGAACAAGUCCAUU-3′ (He et al., 2013); Cep68, 5′-CACCCUCAAAUCACCUACUAA-3′ (Graser et al., 2007b); CP110, 5′-GCAAAACCAGAAUACGAGATT-3′ (Prosser and Morrison, 2015); Neurl-4, 5′-CCAUCAUGCAAGACG GUAA-3′ (Li et al., 2012).

The siRNA oligonucleotides were synthesized by Eurofins MWG Operon and Thermo Fisher Scientific. Transfection of siRNAs was performed with oligofectamine (Thermo Fisher Scientific), following the manufacturer's instructions with a final siRNA concentration of 200 nM. IF assays or Western blots were performed to evaluate the knockdowns efficiency.

Lentiviral shRNA

Lentiviruses were generated using PLKO.1-shscramble-shRNA and pLKO-p53-shRNA-941 (Kim et al., 2007) in 293T cells. We used psPAX2 and pCMV-VSVg as the packaging or envelope plasmid, respectively. We infected RPE-1 cells with the shRNA lentiviruses overnight. To increase the efficiency of viral infection, we added 8 µg/ml polybrene. At 24 h after infection, the selection was performed in 10 µg/ml fresh puromycin-containing media for 10 d. CP110 depletion was validated by IF microscopy.

IF microscopy

hTERT-RPE1 and HFF cells were grown on glass coverslips. Cells were fixed as described with either cold 100% methanol for 5 min, 4% formaldehyde for 10 min, or methanol/acetone (1:1) for 2 min. Cells fixed with formaldehyde were permeabilized with 0.2% Triton X-100 in PBS for 10 min. Before fixation and cilia staining, cells were incubated on ice for 30 min to depolymerize microtubules. Fixed cells were blocked in blocking buffer (2.5% FBS, 0.1% Triton X-100 in PBS) for 1 h and then incubated with primary antibodies for 1 h at room temperature, followed by 1-h incubation with secondary antibodies (Alexa Fluor 488, 594, and 647; Thermo Fisher Scientific). DNA was stained with Hoechst 33342 (Thermo Fisher Scientific) for 2 min. Coverslips were mounted on glass slides using ProLong Gold mounting media (Thermo Fisher Scientific). Cells were imaged with AxioVision software on an inverted Axiovert 200M microscope (NA: 0.55, working distance: 26 mm; ZEISS) equipped with an EC Plan-Neofluar 100×/1.3 oil Ph3 objective. Images were captured with an AxioCam MRm monochrome

digital camera (ZEISS). The distance between centrioles was measured using AxioVision software.

Quantification of cilia and intensities of centriolar proteins

Ciliation rates were calculated from seven to ten randomly selected fields of cells for each experiment. The fluorescence intensity of centrosome markers was determined using ImageJ 1.47v software. A range threshold was applied to specifically select the pixels, showing the signal of the centriole marker. The mean fluorescence intensity was extracted for each immunostained protein.

Rescue experiments using CP110 siRNA

RPE-1 cells were treated either with HsSAS-6 or LRRC45 siRNA for 40 or 28 h, respectively. We then transfected control or CP110 siRNA for 4 h, followed by serum starvation for 24 (LRRC45) or 30 h (HsSAS-6). CP110 depletion was validated using IF microscopy and Western blot analysis.

Western blot analysis

Approximately 4.10^5 cells per condition were lysed for 10 min on ice in NP-40 lysis buffer (150 mM NaCl, 1 mM EDTA, 50 mM Hepes, pH 7.4, and 0.5% NP-40) supplemented with protease inhibitors (2 mM pepstatin and 150 mM aprotinin; both from MP Biochemicals; 1 mM leupeptin; EMD Millipore; 60 µM PMSF; Acros; and 30 µM MG-132; EMD Millipore). Whole-cell extracts were cleared by centrifugation (14,000 rpm, 10 min, 4°C). Protein concentrations were determined by Bradford assay (Bio-Rad). Cell lysates were diluted in Laemmli sample buffer (50 mM Tris HCl, pH 6.8, 10% glycerol, 2% SDS, 1% 2-mercaptoethanol, and 0.1% bromophenol blue) and incubated at 95°C for 5 min to denature proteins. 20 µg total cellular protein were separated by SDS-PAGE and transferred onto a nitrocellulose membrane. The membrane was saturated in 5% milk PBST (5% dry powdered milk, 0.1% Tween-20, and 1× PBS) and incubated in primary antibodies followed by IRDye-conjugated (LI-COR Biosciences) secondary antibodies. Blots were imaged by the LI-COR Biosciences Odyssey SA infrared imaging system. Western blots were quantified using ImageJ 1.47v software ("Gels" command).

Proliferation assay

RPE-1 cells were treated with control or HsSAS-6 siRNA for 48 h followed by plating of 2.5×10^5 cells in a six-well tissue culture plate (Wong et al., 2015). 30 h later, the number of cells was carefully counted and a second passage was performed at the 78-h time point. The number of cells was then analyzed at the 102-h time point. Cells were cultured in serum-rich medium during the whole experiment.

Statistical analysis

Data are reported as arithmetic means ± SEM. Statistical analyses were performed using nonparametric Mann–Whitney test with GraphPad Prism 5 software. Data were generated from at least three independent experiments, unless otherwise indicated. $P \leq 0.05$ was used as the cutoff for statistical significance.

Online supplemental material

Fig. S1 shows that HsSAS-6 depletion generates monocentriolar cells that do not arrest in G1. Fig. S2 shows that LRRC45 depletion disrupts centriole cohesion without up-regulating p53. Fig. S3 confirms that daughter centriole manipulations do not alter basal body association of selected marker proteins. Fig. S4 shows Neurl-4 depletion at the daughter centriole. Fig. S5 shows that Neurl-4 translocates from the daughter to the mother centriole before axoneme extension in HFFs.

Acknowledgments

We thank Drs. Brian Dynlacht, Michel Bornens, and Mikiko Takahashi for the gift of reagents. We are grateful to Drs. Ming Tan, Naomi Morrissette, and Scott Atwood for critical reading of the manuscript.

This work was supported by National Institute of General Medical Sciences grant R01GM089913 (to C. Sütterlin).

The authors declare no competing financial interests.

Author contributions: A. Loukil designed, performed, and analyzed all experiments, prepared the figures, and cowrote the manuscript. K. Tormanen prepared viruses and infected cells. C. Sütterlin designed the experiments, analyzed and discussed the results, and cowrote the manuscript.

Submitted: 30 August 2016
Revised: 29 December 2016
Accepted: 28 February 2017

References

Al-Hakim, A.K., M. Bashkurov, A.-C. Gingras, D. Durocher, and L. Pelletier. 2012. Interaction proteomics identify NEURL4 and the HECT E3 ligase HERC2 as novel modulators of centrosome architecture. *Mol. Cell. Proteomics.* 11:014233. http://dx.doi.org/10.1074/mcp.M111.014233

Al Jord, A., A.-I. Lemaître, N. Delgehyr, M. Faucourt, N. Spassky, and A. Meunier. 2014. Centriole amplification by mother and daughter centrioles differs in multiciliated cells. *Nature.* 516:104–107.

Anderson, C.T., and T. Stearns. 2009. Centriole age underlies asynchronous primary cilium growth in mammalian cells. *Curr. Biol.* 19:1498–1502. http://dx.doi.org/10.1016/j.cub.2009.07.034

Augustin, A., C. Spenlehauer, H. Dumond, J. Ménissier-De Murcia, M. Piel, A.-C. Schmit, F. Apiou, J.-L. Vonesch, M. Kock, M. Bornens, and G. De Murcia. 2003. PARP-3 localizes preferentially to the daughter centriole and interferes with the G1/S cell cycle progression. *J. Cell Sci.* 116:1551–1562. http://dx.doi.org/10.1242/jcs.00341

Bahe, S., Y.-D. Stierhof, C.J. Wilkinson, F. Leiss, and E.A. Nigg. 2005. Rootletin forms centriole-associated filaments and functions in centrosome cohesion. *J. Cell Biol.* 171:27–33. http://dx.doi.org/10.1083/jcb.200504107

Basten, S.G., and R.H. Giles. 2013. Functional aspects of primary cilia in signaling, cell cycle and tumorigenesis. *Cilia.* 2:6. http://dx.doi.org/10.1186/2046-2530-2-6

Basten, S.G., S. Willekers, J.S. Vermaat, G.G. Slaats, E.E. Voest, P.J. van Diest, and R.H. Giles. 2013. Reduced cilia frequencies in human renal cell carcinomas versus neighboring parenchymal tissue. *Cilia.* 2:2. http://dx.doi.org/10.1186/2046-2530-2-2

Boettcher, M., and M.T. McManus. 2015. Choosing the right tool for the job: RNAi, TALEN, or CRISPR. *Mol. Cell.* 58:575–585. http://dx.doi.org/10.1016/j.molcel.2015.04.028

Cizmecioglu, O., M. Arnold, R. Bahtz, F. Settele, L. Ehret, U. Haselmann-Weiss, C. Antony, and I. Hoffmann. 2010. Cep152 acts as a scaffold for recruitment of Plk4 and CPAP to the centrosome. *J. Cell Biol.* 191:731–739. http://dx.doi.org/10.1083/jcb.201007107

Conduit, P.T., A. Wainman, and J.W. Raff. 2015. Centrosome function and assembly in animal cells. *Nat. Rev. Mol. Cell Biol.* 16:611–624. http://dx.doi.org/10.1038/nrm4062

Conroy, P.C., C. Saladino, T.J. Dantas, P. Lalor, P. Dockery, and C.G. Morrison. 2012. C-NAP1 and rootletin restrain DNA damage-induced centriole splitting and facilitate ciliogenesis. *Cell Cycle.* 11:3769–3778. http://dx.doi.org/10.4161/cc.21986

D'Angiolella, V., V. Donato, S. Vijayakumar, A. Saraf, L. Florens, M.P. Washburn, B. Dynlacht, and M. Pagano. 2010. SCF(Cyclin F) controls centrosome homeostasis and mitotic fidelity through CP110 degradation. *Nature.* 466:138–142. http://dx.doi.org/10.1038/nature09140

David, A., F. Liu, A. Tibelius, J. Vulprecht, D. Wald, U. Rothermel, R. Ohana, A. Seitel, J. Metzger, R. Ashery-Padan, et al. 2014. Lack of centrioles and primary cilia in STIL(-/-) mouse embryos. *Cell Cycle.* 13:2859–2868. http://dx.doi.org/10.4161/15384101.2014.946830

Delgehyr, N., J. Sillibourne, and M. Bornens. 2005. Microtubule nucleation and anchoring at the centrosome are independent processes linked by ninein function. *J. Cell Sci.* 118:1565–1575. http://dx.doi.org/10.1242/jcs.02302

Dormoy, V., K. Tormanen, and C. Sütterlin. 2013. Par6γ is at the mother centriole and controls centrosomal protein composition through a Par6α-dependent pathway. *J. Cell Sci.* 126:860–870. http://dx.doi.org/10.1242/jcs.121186

Fang, G., D. Zhang, H. Yin, L. Zheng, X. Bi, and L. Yuan. 2014. Centlein mediates an interaction between C-Nap1 and Cep68 to maintain centrosome cohesion. *J. Cell Sci.* 127:1631–1639. http://dx.doi.org/10.1242/jcs.139451

Flanagan, A.-M., E. Stavenschi, S. Basavaraju, D. Gaboriau, D.A. Hoey, and C.G. Morrison. 2017. Centriole splitting caused by loss of the centrosomal linker protein C-NAP1 reduces centriolar satellite density and impedes centrosome amplification. *Mol. Biol. Cell.* 28:736–745. http://dx.doi.org/10.1091/mbc.E16-05-0325

Fliegauf, M., T. Benzing, and H. Omran. 2007. When cilia go bad: Cilia defects and ciliopathies. *Nat. Rev. Mol. Cell Biol.* 8:880–893. http://dx.doi.org/10.1038/nrm2278

Fong, C.S., G. Mazo, T. Das, J. Goodman, M. Kim, B.P. O'Rourke, D. Izquierdo, and M.-F.B. Tsou. 2016. 53BP1 and USP28 mediate p53-dependent cell cycle arrest in response to centrosome loss and prolonged mitosis. *eLife.* 5:e16270. http://dx.doi.org/10.7554/eLife.16270

Fu, J., I.M. Hagan, and D.M. Glover. 2015. The centrosome and its duplication cycle. *Cold Spring Harb. Perspect. Biol.* 7:a015800. http://dx.doi.org/10.1101/cshperspect.a015800

Gerdes, J.M., E.E. Davis, and N. Katsanis. 2009. The vertebrate primary cilium in development, homeostasis, and disease. *Cell.* 137:32–45. http://dx.doi.org/10.1016/j.cell.2009.03.023

Gillingham, A.K., and S. Munro. 2000. The PACT domain, a conserved centrosomal targeting motif in the coiled-coil proteins AKAP450 and pericentrin. *EMBO Rep.* 1:524–529. http://dx.doi.org/10.1093/embo-reports/kvd105

Goetz, S.C., and K.V. Anderson. 2010. The primary cilium: A signalling centre during vertebrate development. *Nat. Rev. Genet.* 11:331–344. http://dx.doi.org/10.1038/nrg2774

Goetz, S.C., K.F. Liem Jr., and K.V. Anderson. 2012. The spinocerebellar ataxia-associated gene Tau tubulin kinase 2 controls the initiation of ciliogenesis. *Cell.* 151:847–858. http://dx.doi.org/10.1016/j.cell.2012.10.010

Gradilone, S.A., B.N. Radtke, P.S. Bogert, B.Q. Huang, G.B. Gajdos, and N.F. LaRusso. 2013. HDAC6 inhibition restores ciliary expression and decreases tumor growth. *Cancer Res.* 73:2259–2270. http://dx.doi.org/10.1158/0008-5472.CAN-12-2938

Graser, S., Y.-D. Stierhof, S.B. Lavoie, O.S. Gassner, S. Lamla, M. Le Clech, and E.A. Nigg. 2007a. Cep164, a novel centriole appendage protein required for primary cilium formation. *J. Cell Biol.* 179:321–330. http://dx.doi.org/10.1083/jcb.200707181

Graser, S., Y.-D. Stierhof, and E.A. Nigg. 2007b. Cep68 and Cep215 (Cdk5rap2) are required for centrosome cohesion. *J. Cell Sci.* 120:4321–4331. http://dx.doi.org/10.1242/jcs.020248

Hassounah, N.B., R. Nagle, K. Saboda, D.J. Roe, B.L. Dalkin, and K.M. McDermott. 2013. Primary cilia are lost in preinvasive and invasive prostate cancer. *PLoS One.* 8:e68521. http://dx.doi.org/10.1371/journal.pone.0068521

He, R., N. Huang, Y. Bao, H. Zhou, J. Teng, and J. Chen. 2013. LRRC45 is a centrosome linker component required for centrosome cohesion. *Cell Reports.* 4:1100–1107. http://dx.doi.org/10.1016/j.celrep.2013.08.005

Hilgendorf, K.I., C.T. Johnson, and P.K. Jackson. 2016. The primary cilium as a cellular receiver: Organizing ciliary GPCR signaling. *Curr. Opin. Cell Biol.* 39:84–92. http://dx.doi.org/10.1016/j.ceb.2016.02.008

Ishikawa, H., and W.F. Marshall. 2011. Ciliogenesis: Building the cell's antenna. *Nat. Rev. Mol. Cell Biol.* 12:222–234. http://dx.doi.org/10.1038/nrm3085

Ishikawa, H., A. Kubo, S. Tsukita, and S. Tsukita. 2005. Odf2-deficient mother centrioles lack distal/subdistal appendages and the ability to generate primary cilia. *Nat. Cell Biol.* 7:517–524. http://dx.doi.org/10.1038/ncb1251

Januschke, J., J. Reina, S. Llamazares, T. Bertran, F. Rossi, J. Roig, and C. Gonzalez. 2013. Centrobin controls mother-daughter centriole asymmetry in Drosophila neuroblasts. *Nat. Cell Biol.* 15:241–248. http://dx.doi.org/10.1038/ncb2671

Kim, S., and B.D. Dynlacht. 2013. Assembling a primary cilium. *Curr. Opin. Cell Biol.* 25:506–511. http://dx.doi.org/10.1016/j.ceb.2013.04.011

Kim, J.-S., C. Lee, C.L. Bonifant, H. Ressom, and T. Waldman. 2007. Activation of p53-dependent growth suppression in human cells by mutations in PTEN or PIK3CA. *Mol. Cell. Biol.* 27:662–677. http://dx.doi.org/10.1128/MCB.00537-06

Kobayashi, T., and B.D. Dynlacht. 2011. Regulating the transition from centriole to basal body. *J. Cell Biol.* 193:435–444. http://dx.doi.org/10.1083/jcb.201101005

Kuhns, S., K.N. Schmidt, J. Reymann, D.F. Gilbert, A. Neuner, B. Hub, R. Carvalho, P. Wiedemann, H. Zentgraf, H. Erfle, et al. 2013. The microtubule affinity regulating kinase MARK4 promotes axoneme extension during early ciliogenesis. *J. Cell Biol.* 200:505–522. http://dx.doi.org/10.1083/jcb.201206013

Lambrus, B.G., V. Daggubati, Y. Uetake, P.M. Scott, K.M. Clutario, G. Sluder, and A.J. Holland. 2016. A USP28-53BP1-p53-p21 signaling axis arrests growth after centrosome loss or prolonged mitosis. *J. Cell Biol.* 214:143–153. http://dx.doi.org/10.1083/jcb.201604054

Lechtreck, K.F. 2015. IFT-cargo interactions and protein transport in cilia. *Trends Biochem. Sci.* 40:765–778. http://dx.doi.org/10.1016/j.tibs.2015.09.003

Leidel, S., M. Delattre, L. Cerutti, K. Baumer, and P. Gönczy. 2005. SAS-6 defines a protein family required for centrosome duplication in *C. elegans* and in human cells. *Nat. Cell Biol.* 7:115–125. http://dx.doi.org/10.1038/ncb1220

Li, J., S. Kim, T. Kobayashi, F.-X. Liang, N. Korzeniewski, S. Duensing, and B.D. Dynlacht. 2012. Neurl4, a novel daughter centriole protein, prevents formation of ectopic microtubule organizing centres. *EMBO Rep.* 13:547–553. http://dx.doi.org/10.1038/embor.2012.40

Li, J., V. D'Angiolella, E.S. Seeley, S. Kim, T. Kobayashi, W. Fu, E.I. Campos, M. Pagano, and B.D. Dynlacht. 2013. USP33 regulates centrosome biogenesis via deubiquitination of the centriolar protein CP110. *Nature.* 495:255–259. http://dx.doi.org/10.1038/nature11941

Mahjoub, M.R., Z. Xie, and T. Stearns. 2010. Cep120 is asymmetrically localized to the daughter centriole and is essential for centriole assembly. *J. Cell Biol.* 191:331–346. http://dx.doi.org/10.1083/jcb.201003009

Martínez-Noël, G., J.T. Galligan, M.E. Sowa, V. Arndt, T.M. Overton, J.W. Harper, and P.M. Howley. 2012. Identification and proteomic analysis of distinct UBE3A/E6AP protein complexes. *Mol. Cell. Biol.* 32:3095–3106. http://dx.doi.org/10.1128/MCB.00201-12

Mayor, T., Y.-D. Stierhof, K. Tanaka, A.M. Fry, and E.A. Nigg. 2000. The centrosomal protein C-Nap1 is required for cell cycle-regulated centrosome cohesion. *J. Cell Biol.* 151:837–846. http://dx.doi.org/10.1083/jcb.151.4.837

Mazo, G., N. Soplop, W.-J. Wang, K. Uryu, and M.B. Tsou. 2016. Spatial control of primary ciliogenesis by subdistal appendages alters sensation-associated properties of cilia. *Dev. Cell.* 39:424–437. http://dx.doi.org/10.1016/j.devcel.2016.10.006

Menzl, I., L. Lebeau, R. Pandey, N.B. Hassounah, F.W. Li, R. Nagle, K. Weihs, and K.M. McDermott. 2014. Loss of primary cilia occurs early in breast cancer development. *Cilia.* 3:7. http://dx.doi.org/10.1186/2046-2530-3-7

Mikule, K., B. Delaval, P. Kaldis, A. Jurcyzk, P. Hergert, and S. Doxsey. 2007. Loss of centrosome integrity induces p38-p53-p21-dependent G1-S arrest. *Nat. Cell Biol.* 9:160–170. http://dx.doi.org/10.1038/ncb1529

Nigg, E.A. 2002. Centrosome aberrations: Cause or consequence of cancer progression? *Nat. Rev. Cancer.* 2:815–825. http://dx.doi.org/10.1038/nrc924

Panic, M., S. Hata, A. Neuner, and E. Schiebel. 2015. The centrosomal linker and microtubules provide dual levels of spatial coordination of centrosomes. *PLoS Genet.* 11:e1005243. http://dx.doi.org/10.1371/journal.pgen.1005243

Pelletier, L., and Y.M. Yamashita. 2012. Centrosome asymmetry and inheritance during animal development. *Curr. Opin. Cell Biol.* 24:541–546. http://dx.doi.org/10.1016/j.ceb.2012.05.005

Prosser, S.L., and C.G. Morrison. 2015. Centrin2 regulates CP110 removal in primary cilium formation. *J. Cell Biol.* 208:693–701. http://dx.doi.org/10.1083/jcb.201411070

Schmidt, K.N., S. Kuhns, A. Neuner, B. Hub, H. Zentgraf, and G. Pereira. 2012. Cep164 mediates vesicular docking to the mother centriole during early steps of ciliogenesis. *J. Cell Biol.* 199:1083–1101. http://dx.doi.org/10.1083/jcb.201202126

Shpak, M., M.M. Goldberg, and M.C. Cowperthwaite. 2014. Cilia gene expression patterns in cancer. *Cancer Genomics Proteomics.* 11:13–24.

Sillibourne, J.E., I. Hurbain, T. Grand-Perret, B. Goud, P. Tran, and M. Bornens. 2013. Primary ciliogenesis requires the distal appendage component Cep123. *Biol. Open.* 2:535–545. http://dx.doi.org/10.1242/bio.20134457

Sluder, G., and A. Khodjakov. 2010. Centriole duplication: Analogue control in a digital age. *Cell Biol. Int.* 34:1239–1245. http://dx.doi.org/10.1042/CBI20100612

Sonnen, K.F., L. Schermelleh, H. Leonhardt, and E.A. Nigg. 2012. 3D-structured illumination microscopy provides novel insight into architecture of human centrosomes. *Biol. Open.* 1:965–976. http://dx.doi.org/10.1242/bio.20122337

Spektor, A., W.Y. Tsang, D. Khoo, and B.D. Dynlacht. 2007. Cep97 and CP110 suppress a cilia assembly program. *Cell.* 130:678–690. http://dx.doi.org/10.1016/j.cell.2007.06.027

Tanos, B.E., H.-J. Yang, R. Soni, W.-J. Wang, F.P. Macaluso, J.M. Asara, and M.-F.B. Tsou. 2013. Centriole distal appendages promote membrane

docking, leading to cilia initiation. *Genes Dev.* 27:163–168. http://dx.doi.org/10.1101/gad.207043.112

Uhlén, M., E. Björling, C. Agaton, C.A.-K. Szigyarto, B. Amini, E. Andersen, A.-C. Andersson, P. Angelidou, A. Asplund, C. Asplund, et al. 2005. A human protein atlas for normal and cancer tissues based on antibody proteomics. *Mol. Cell. Proteomics.* 4:1920–1932. http://dx.doi.org/10.1074/mcp.M500279-MCP200

Veland, I.R., A. Awan, L.B. Pedersen, B.K. Yoder, and S.T. Christensen. 2009. Primary cilia and signaling pathways in mammalian development, health and disease. *Nephron, Physiol.* 111:39–53. http://dx.doi.org/10.1159/000208212

Veleri, S., S.H. Manjunath, R.N. Fariss, H. May-Simera, M. Brooks, T.A. Foskett, C. Gao, T.A. Longo, P. Liu, K. Nagashima, et al. 2014. Ciliopathy-associated gene Cc2d2a promotes assembly of subdistal appendages on the mother centriole during cilia biogenesis. *Nat. Commun.* 5:4207. http://dx.doi.org/10.1038/ncomms5207

Wong, Y.L., J.V. Anzola, R.L. Davis, M. Yoon, A. Motamedi, A. Kroll, C.P. Seo, J.E. Hsia, S.K. Kim, J.W. Mitchell, et al. 2015. Reversible centriole depletion with an inhibitor of Polo-like kinase 4. *Science.* 348:1155–1160. http://dx.doi.org/10.1126/science.aaa5111

Wu, K.-S., and T.K. Tang. 2012. CPAP is required for cilia formation in neuronal cells. *Biol. Open.* 1:559–565. http://dx.doi.org/10.1242/bio.20121388